Shape of polygonal quantum dots and ground-state instability in the spin polarization

Masamu Ishizuki, Hannyo Takemiya, Takuma Okunishi, and Kyozaburo Takeda*
Graduate School of Advanced Science and Engineering, Waseda University, Tokyo 169-8555, Japan

Kouichi Kusakabe
Graduate School of Engineering Science, Osaka University, Osaka 560-8531, Japan
(Received 14 November 2011; revised manuscript received 14 February 2012; published 18 April 2012)

We theoretically investigate the ground-state electronic structure and the spin polarization of four electrons confined in two-dimensional (2D) polygonal quantum dots. We employ standard mean-field theory approaches using unrestricted Hartree–Fock (UHF) and density functional theory (DFT) calculations. Resonant UHF configuration interaction (res-UHF CI) calculations were also performed to incorporate the electron correlation more intuitively. Odd polygons (trigons and pentagons) preferentially generate the ground-state triplet as predicted by Hund's rule, whereas even polygons (tetragons, hexagons, and octagons) promote ground-state instability in the spin multiplicity and tend to produce an anti-Hund state of the ground-state singlet with strengthening of the interelectron interaction. The circle, a limited polygon having an infinite number of apexes, divides these odd and even polygons, and the ground-state instability can be well classified by the area of the polygon apexes that protrudes from an equisized circle.

DOI: 10.1103/PhysRevB.85.155316 PACS number(s): 73.21.La, 73.22.Gk

I. INTRODUCTION

Since the first fabrication of quantum dots (QDs),[1,2] advances in semiconductor nanotechnology have enabled QDs with diverse morphologies to be fabricated. By artificially controlling the electronic shell structures of these QDs, experimentalists have found several novel and important phenomena caused by the interelectron interaction.[3,4] Theoreticians have carried out their "gedankenexperiments" to reveal the inherent nature of many-electron system. Synergy between these experiments and theories further accelerates the research development in these areas. The two-dimensional (2D) QD system is particulary important for theoretical study because this system serves as a theoretical model to deepen our understandings on the complicated many-electron state system.[5,6] Bryant was first to calculate the ground-state electronic structure of the square QD (SQD) system, including the electron correlation via the configuration interaction (CI) technique.[7] Since then, several crucial works have been carried out (see Reimann and Manninen[8] for a comprehensive review).

The relationship between the spin state and the interelectron interaction is one of the fundamental problems in the ground state of these 2D QD systems. Koskinen *et al.*[9] studied the electronic structures and spin states of a QD system with a 2D harmonic potential by varying the number of confined electrons ($N = 2$–46). They performed density functional theory (DFT) calculations using the local spin-density approximation (LSDA) and found that the resulting total spin S agrees with that predicted by Hund's rule when the system has a small confinement area. They also found a few spin isomers with total spin of zero ($S = 0$) that have slightly higher energies than the ground-state configuration. Intriguingly, they discovered that one of these completely unpolarized states has an even lower energy than the Hund state ($S = 2$, $N = 24$, 34). Thus they conjectured that an anti-Hund state of the ground-state singlet ($N = 24$ and 34) may exist, whose space-dependent spin polarization exhibits spatial oscillations similar to spin-density waves (SDWs) in bulk systems.[10] Yannouleas and Landman[11] also confirmed the existence of the same SDW ground states by performing spin-and-space unrestricted Hartree-Fock (UHF) calculations. They conjectured that these SDW ground states result from spontaneous symmetry breaking. In contrast, Hirose and Wingreen[12] used exact diagonalization to demonstrate that the SDW ground states result from an unphysical mixture between states with different total spins. They concluded that these anti-Hund states are artifacts of broken spin symmetry due to mean-field theory (MFT). However, Hirose and Wingreen[12] further suggested that Hund's rule may be violated based on their observation of the spin-unpolarized ground state of $S = 0$, $L_z = 0$ when they varied the confinement potential to give a larger splitting in the single-particle energies at higher angular momentum.

Similar studies for the 2D square QD system have been carried out by Austing *et al.*,[13] who considered the effect of ellipsoidal deformation on the electronic level structure and magnetism of QDs both theoretically and experimentally. They predicted a spin triplet-singlet transition in accordance with the deformation of the circular QD. Creffield *et al.*[14] have carried out the first EDM study of the electronic structure for the polygonal QD system of triangle, square, and hexagon. They examined the behavior of the lowest-energy levels of two electrons confined to 2D polygonal QDs, and found the quasicrystalline structure in the ground-state charge distribution for sufficiently large QDs. They also discussed the magnetic field dependence of the low-energy spectrum of the two-electron square QD system.[15] Nieminen's group studied the electronic structures and related properties of these 2D QD systems extensively and systematically. Räsänen *et al.*[16] have studied the square and rectangular QD systems intensively by using the spin-density-functional theory (SDFT) and quantum Monte Carlo methods, demonstrating that the electronic structure is very sensitive to the shape of the QD and that the $S = 1$ state in rectangular QDs is bracketed by SDW-like solutions. They also discussed the effect of an external magnetic field for 2D rectangular QDs having a

hard-wall potential.[17] Their DFT study has been further extended on the formation of Wigner molecules in the polygonal QDs of triangle, square, pentagon, and hexagon, where they have carefully investigated the two-electron singlet state by comparing the symmetry-broken SDFT ground state with the symmetry-preserved DFT solutions.[6,18] The problem of broken symmetry in the DFT approach has also been studied by Harju *et al.*[5] of the Nieminen group by performing the exact diagonalization computations alongside with the DFT calculations.

These theoretical studies indicate that the electron correlation needs to be considered in order to determine quantitative details of the ground-state electronic structure and spin state when the interelectron interaction is strengthened. Nevertheless, in the present study, we carry out the UHF and DFT calculations of the MFT approach, because our current purpose is not to reveal quantitative details of the electronic structures but rather to investigate the relationship between the spin multiplicity of the ground state and the morphology of 2D QDs systematically. The MFT approach can give "consistent" results in terms of crude estimates only for the energetic stabilities of the Hund and anti-Hund states.[8,26] Accordingly, we focus on 2D polygonal QDs, whose apexes (M) equal to 3 (trigon), 4 (tetragon), 5 (pentagon), 6 (hexagon), and 8 (octagon).[19] We also consider a circle, which is a limited polygon having an infinite number of apexes. We seek to clarify the differences resulting from the apex shapes of these polygons. Consequently, we surround the polygons with an infinite potential barrier (a hard wall) rather than the harmonic potential, as the wave function confined by the latter penetrates the harmonic wall. This will accurately model the detailed differences of the morphologies and apex shapes of polygons. We here discuss the four-electron system of $N(= N^{\alpha} + N^{\beta}) = 4$. This number is the minimum confined electrons required to represent all Coulomb interactions (including all direct and exchange terms), because 2D polygonal and circular QDs generate the nondegenerate single-electron ground state $(n,l) = (0,0)$, whereas the first excited one is doubly degenerate $(n,l) = (0, \pm 1)$.[20] Thus the straightforward application of Hund's rule predicts a triplet ground state for the four electrons confined in the above-mentioned 2D polygons irrespective of the apex number M. As such, the present study qualitatively (but systematically) discusses the applicability of Hund's first rule to polygons. To numerically determine the ground state, we examine the energetics of a four-electron system by varying the spin configuration between the fully spin-unpolarized ($|N^{\alpha} - N^{\beta}| = 0$; singlet, S) and spin-polarized ($|N^{\alpha} - N^{\beta}| = 2$; triplet, T) states and by changing the polygon size.

II. CALCULATIONAL METHODOLOGY

Both the coupled UHF and Kohn-Sham[21,22] DFT/LSDA equations are solved numerically by the finite difference method in which the wave function is discretized into real space grid points. A Cartesian (x and y) mesh is employed for the systematic execution of the finite difference method. However, we vary the number of mesh divisions based on the polygon. We adopted a real-space grid method with 32×32 mesh points for most polygons ($M > 4$; including circles) because this mesh well represents the apex shapes and the single-electron wave functions confined within the polygon. However, regular and modified trigons require finer meshes; for example, in Kubota trigons we employed a 90×90 mesh to reproduce their extremely narrow apexes. We also assume that the present SQDs are fabricated by GaAs and have an effective mass of $m^* = 0.067 m_e$ and a relative permittivity $\epsilon^* = 12.52$, resulting in an effective Bohr radius of $a_B^* = 9.90$ nm. Accordingly, the energy is scaled by the effective atomic unit (a.u.), $2\mathrm{Ry}^* = m^* e^4/\hbar^2\epsilon = 11.61$ meV. The details of the calculations have been reported elsewhere.[23]

III. TETRAGON AND TRIGON

We begin our discussion with the four electrons confined in the 2D regular tetragon, which is surrounded by an infinite hard wall and has a point group symmetry of D_{4h}. We compare the total energies of the lowest spin-singlet (E^{S}) and spin-triplet (E^{T}) states in Fig. 1(a),[24] where we plot the difference $\Delta E^{\mathrm{ST}} = E^{\mathrm{S}} - E^{\mathrm{T}}$ against the confinement length L. Accordingly, a positive value in Fig. 1(a) indicates the triplet stable and a negative value indicates the singlet stable (S/T profile). The UHF approach (red line) demonstrates that the four electrons confined in the regular tetragon produce the ground-state triplet (spin polarized, $|N^{\alpha} - N^{\beta}| = 2$) when the confinement length is sufficiently small ($L = 2$ a.u., for example). This feature is well consistent with Hund's rule, because the geometrical symmetry of D_{4h} conserves the degeneracy in the first excited (single-electron) states (e_u). However, Fig. 1(a) indicates that the total-energy difference ΔE^{ST} drops to almost zero at $L \sim 3$ indicating instability between the singlet and triplet states (S/T instability). Furthermore, one finds a negative value of ΔE^{ST} when $L > 4$. This means that in this range the ground state singlet is energetically preferable (spin unpolarized, $|N^{\alpha} - N^{\beta}| = 0$) and Hund's rule is violated. Figure 1(a) also indicates that this UHF ground-state singlet is most stable around $L \sim 4$ and becomes less favorable as L increases. Also, apparent is the spin-singlet and spin-triplet states become energetically degenerate when L is infinite. Quite similar results are also obtained from the DFT/LSDA calculation [green line in Fig. 1(a)]. The partial inclusion of the electron correlation via the DFT "*exchange-correlation*" term extends the Hund state of the ground-state triplet until $L = 6$.[25] However, the energy difference ΔE^{ST} likewise crosses the zero line, indicating the anti-Hund state of the ground-state singlet. Thus both MFT approaches (UHF and DFT) demonstrate that the four-electron system confined in the regular tetragon changes its ground state spin-polarization from ferromagnetic (spin-triplet, $|N^{\alpha} - N^{\beta}| = 2$) to antiferromagnetic (spin-singlet, $|N^{\alpha} - N^{\beta}| = 0$) as the interelectron Coulomb interaction grows stronger.[24]

Ignoring the commonly known drawbacks of the UHF method (namely, spin contamination and lack of electron correlation), we qualitatively analyze the resulting spin-polarization distribution. Figure 1(b) gives the calculated spin density for the spin singlet ($|N^{\alpha} - N^{\beta}| = 0$) and triplet ($|N^{\alpha} - N^{\beta}| = 2$), respectively. One should note that the UHF ground-state singlet generates an alternating spatial oscillation in accordance with the spin direction (at $L = 6$, for example). Thus spin-up and spin-down states result locally while the system is completely unpolarized ($|N^{\alpha} - N^{\beta}| = 0$, $S = 0$). Accordingly, the fourfold rotational axis C_4 found in the

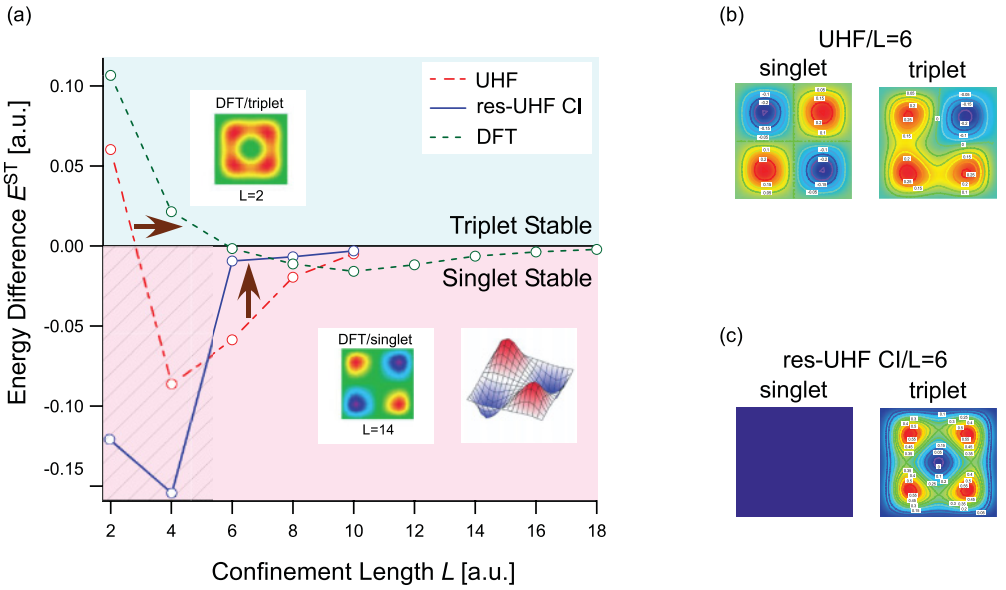

FIG. 1. (Color online) Comparison of the total energies of four electrons confined in a regular tetragon (D_{4h}) with an area of $L \times L$(a).[24] To calculate the total energy, we considered two spin states: singlet (unpolarized; $|N^{\alpha} - N^{\beta}| = 0$) and triplet (polarized; $|N^{\alpha} - N^{\beta}| = 2$), and employed the MFT approaches of UHF (red) and DFT (green). We also give the S/T profile calculated by the res-UHF CI method (blue). However, in the hatched region of $L < 5$, the present res-UHF CI method gives rather inconsistent results due to the poor basis sets of scf(self-consistent)-UHF Slater solutions because the strong confinement allows the scf solutions to be the same. The figure shows the resulting UHF spin densities ($L = 6$) for the unpolarized and polarized states calculated by the (b) UHF and (c) res-UHF CI methods. The res-UHF CI calculation demonstrates that the resulting zero spin is uniformly distributed with no spatial oscillations in the spin up and spin down (see inset), whereas the apparent SDWs are given by the UHF results. The calculated expectation value for the angular moment is exactly $\langle L_z \rangle = 0.000$.

total electron density now becomes the twofold one in the spin density. In contrast, the lowest UHF triplet state is no longer the ground state [$L = 6$, Fig. 1(b)], so it does not lead to any rotational symmetries in the spin density. The DFT results exhibit similar characteristics. The strong confinement ($L = 2$) causes the Hund state of the ground-state triplet, where the spins are polarized. In this, the fourfold rotational symmetry in the D_{4h} Hamiltonian is well preserved both in the spin and total electron densities [see Fig. 1(a)]. However, the spin density oscillates spatially in the DFT ground-state singlet (at $L = 14$, for example) as shown in the inset of Fig. 1(a).

These characteristics are highly consistent with those found by Koskinen *et al.*,[9] and Yannouleas and Landman.[11] However, as Hirose and Wingreen[12] concluded, the anti-Hund state of the ground-state singlet, which has the SDW, is an artifact of the broken spin symmetry due to the mean-field theory, being an unphysical mixture of states of different total spin. We have, therefore, included the electron correlation to improve this symmetry breaking and to find the correct ground state. For this subject, we have carried out the multireference configuration interaction (CI) treatment by employing the resonant UHF configuration interaction (res-UHF CI) method,[27–29] which approximates a many-body wave function by the superposition of nonorthogonal Slater determinants. Figure 1(c) illustrates the spin density for the lowest spin-singlet and spin-triplet states obtained by the res-UHF CI calculations. The unpolarized spin-zero state extends uniformly to cause the spin singlet whereas the fourfold rotation is found in the spin triplet [see Fig. 1(c)]. Thus the inclusion of the electron correlation through the res-UHF CI treatment removes the symmetry breaking and restores the symmetry of the Hamiltonian for both the spin-singlet and spin-triplet states. Nevertheless, what one should note is that the spin-unpolarized anti-Hund state ($|N^{\alpha} - N^{\beta}| = 0$) is still more energetically stable than the spin-polarized Hund state ($|N^{\alpha} - N^{\beta}| = 2$) when the confinement is weakened [blue line in Fig. 1(a)]. Thus the crude estimates given by the MFT approaches (UHF and DFT calculations) still give empirically consistent results in terms of the relative energetic stabilities of the Hund and anti-Hund states.[8,26]

What ground state do the four electrons cause when they are confined in the 2D trigonal QD? Figure 2(a) shows the corresponding UHF S/T profile when the four electrons are confined in the regular trigon ($M = 3$) having a point group symmetry of D_{3h} as a function of the confinement area $\mathcal{A} = (L^*)^2$. The resulting positive value of ΔE^{ST} [see Fig. 2(a)] indicates that the four electrons always prefer the ground-state triplet and their spins are polarized to be ferromagnetic. This finding is well consistent with the Hund rule, but it differs from the above-mentioned result for a square QD.

Figure 2(b) gives the resulting spin density for the spin-singlet ($|N^{\alpha} - N^{\beta}| = 0$) and spin-triplet ($|N^{\alpha} - N^{\beta}| = 2$) states. For the trigonal confinement, three peaks appear at the apex edges in larger trigons, irrespective to the spin-singlet and spin-triplet states. For the singlet state, the remaining one electron causes a peak at the space, but destroys the geometrical symmetry of the trigonal Hamiltonian. Accordingly, the spin-singlet distribution is unnatural, and the lowest spin-singlet state of $N^{\alpha} - N^{\beta} = 0$ is no longer the ground state although an "SDW-like" distribution might appear. Contrary, the triplet state places the remaining electron (having the opposite spin) at the center as shown in Fig. 2(b). This

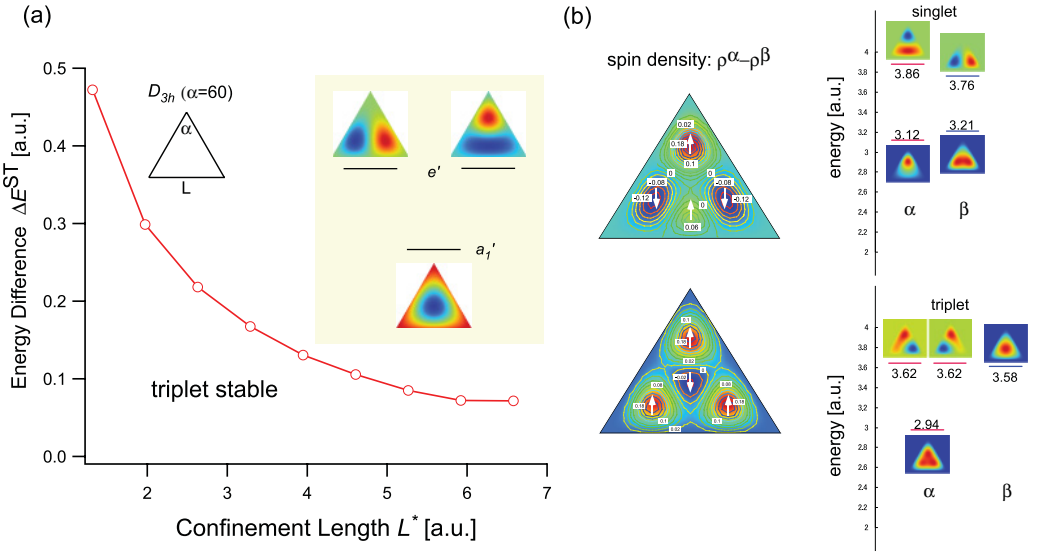

FIG. 2. (Color online) (a) UHF S/T profile for four electrons confined in a regular triangle (D_{3h}) as a function of the effective confinement length $L^* = \frac{4\sqrt{3}}{2}L$, where L is the base line of the regular triangle. (b) The resulting spin density for the spin-singlet (unpolarized; $|N^\alpha - N^\beta| = 0$) and spin-triplet (polarized; $|N^\alpha - N^\beta| = 2$) states with the corresponding scf-MOs of these four electrons (see also Appendix A).

distribution is natural to maintain the geometrical symmetry of the trigonal Hamiltonian. Consequently, the ground state of the trigon is the Hund state of $|N^\alpha - N^\beta| = 2$ (triplet) with having the "reasonable" space-dependent spin polarization shown in Fig. 2(b); α (β) spins localize at the three apex edges while a β (α) spin localizes at the center. This feature is consistent with the state suggested by the Ising spin model.[30] Therefore it can be simply said that these characteristics are caused by the difference/agreement in the number of confined electrons ($N = 4$) and the number of apexes (M). The difference of $N = 4$ and $M = 3$ in trigon prefers the ground-state triplet due to the rational spin distribution, whereas the agreement of $N = 4$ and $M = 4$ in tetragon causes the ground S/T instability in tetragon (see Appendix B). However, the resulting zero approach in ΔE^{ST} both in trigon and tetragon consistently demonstrate the energetical degeneracy between these spin-singlet and spin-triplet states in the finite length ($L = \infty$).

IV. POLYGONS

Four electrons confined in a trigon ($M = 3$) generate the Hund state of the ground-state triplet ($|N^\alpha - N^\beta| = 2$), whereas four electrons confined in a tetragon ($M = 4$) can change the ground state from a spin-polarized (Hund) state to a spin-unpolarized (anti-Hund) state ($|N^\alpha - N^\beta| = 0$) with increasing interelectron interaction strength. These results raise the possibility that odd polygons (with an odd number of apexes) generate the Hund ground state, whereas even polygons (with an even number of apexes) prefer the anti-Hund ground state. To explore this, we extended our calculations to other polygons (namely, pentagon, hexagon, octagon, and circle).[31] Figure 3 shows the S/T profiles of these 2D polygons as functions of their confinement areas $\mathcal{A} = (L^*)^2$.

When the four electrons are confined in the even polygons [hexagon ($M = 6$), octagon ($M = 8$), and the previously shown tetragon ($M = 4$)], they energetically prefer the ground-state triplet ($|N^\alpha - N^\beta| = 2$) under strong confinement, consistent with Hund's rule. However, with an expansion of the confinement area $\mathcal{A}$ (increase in L^*), the total-energy difference ΔE^{ST} becomes almost zero at the critical length L^{ST} (where $\Delta E^{\mathrm{ST}} = 0$) and the singlet/triplet (S/T) instability is generated. A further increase in L^* changes the value of ΔE^{ST} to negative. Consequently, the four-electron system in the even polygons has the potential to cause the ground-state singlet

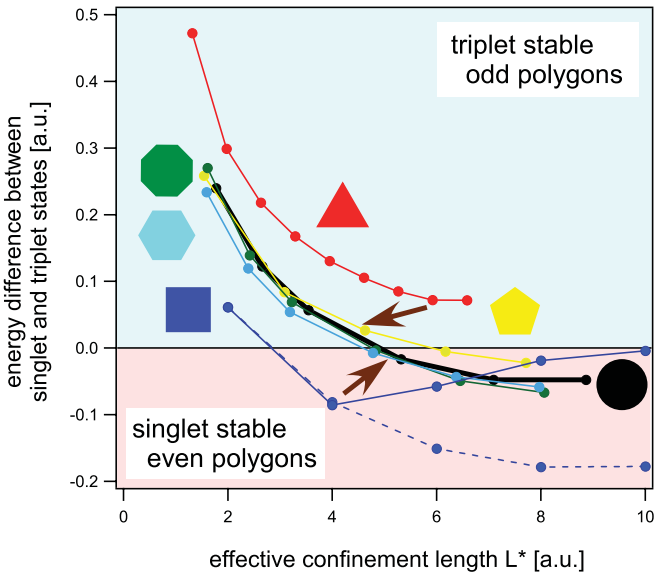

FIG. 3. (Color online) S/T profiles for tetragon, hexagon, and octagon (even polygons) and for trigon and pentagon (odd polygons) obtained by the UHF calculation. L^* indicates the effective confinement length defined by $L^* = \mathcal{A}$, where $\mathcal{A}$ represents the confinement areas of these 2D polygons. For the tetragon, we compared the scf solutions by employing two sets of the initial states; one from the single-electron eigenstates (broken line) and the other is those obtained by the two-electrons scf eigenstates (solid line).

($|N^{\alpha} - N^{\beta}| = 0$). One should further note that the preference for the anti-Hund ground state in even polygons decreases with increasing apex number M. Accordingly, the critical confinement length L^{ST} increases with an increase in M. As a result, the S/T profiles for the even polygons approaches that of the circular system as the number of apexes M increases (demonstrated in Fig. 3).

In contrast, four electrons confined in odd polygons (namely, trigon $M = 3$ and pentagon $M = 5$) have a greater preference for the Hund state of the ground-state triplet than four electrons confined in even polygons with the same confinement area $\mathcal{A}$ (L^*). Figure 3 shows that the Hund state of the ground-state triplet exists until $L^* = 6$ for a pentagon. It also shows that the S/T profiles for odd polygons approaches that of a circle with increasing number of apexes M. In other words, the critical confinement length L^{ST} for odd polygons decreases with increasing M. Thus odd polygons (trigon, pentagon) prefer to generate the ground state triplet as predicted by Hund's rule, whereas even polygons (tetragon, hexagon, octagon) cause ground-state instability in the spin multiplicity and tend to produce the anti-Hund state of the ground-state singlet with strengthening of the interelectron interaction. The circle, which has an infinite number of apexes ($M = \infty$), is intermediate between these two cases.

V. MODIFIED TRIGONS

Figure 3 shows that the spin multiplicity for the four-electron ground state strongly depends on the number of apexes M, i.e., it depends on the shape of the polygon (M) as well as its size $\mathcal{A} = (L^*)^2$. Here, we discuss the shape and size of the confinement area by studying a regular trigon and its derivatives, because the four electrons confined in the regular trigon uniformly generate the consistent Hund state of the ground-state triplet ($|N^{\alpha} - N^{\beta}| = 2$) (see Fig. 2). The modified trigons considered are formed by curves of constant width whose diameters d are the same for any point on the opposite side [see Fig. 4(a)]. There are two well-known modified trigons: the Reuleaux trigon and Kubota trigon [see Fig. 4(a)]. The Reuleaux trigon has convex sides; whereas the Kubota trigon has concave sides. Consequently, the apexes of a Reuleaux trigon have larger angles than those of a regular trigon, whereas the apexes of Kubota trigon are narrower. Both of these modified trigons, though, have the same point group symmetry (D_{3h}) as a regular trigon. Their S/T profiles [see Fig. 4(b)] indicate that four electrons confined in both Reuleaux and Kubota trigons give the Hund state of the ground-state triplet, similar to that for a regular trigon. One should note that a Kubota trigon enhances the preference for the Hund ground state, whereas a Reuleaux trigon weakens it. A regular trigon is intermediate between the two modified trigons, provided the confinement area $\mathcal{A}$ remains the same.

In Fig. 4(c), we replot the S/T profiles for Reuleaux and Kubota trigons against the diameter d. When Reuleaux and Kubota trigons have the same diameter d, they will have the same interelectron Coulomb energy because the Coulomb interaction is determined by the interelectron distances of the confined electrons (if the extensions of the apexes and the difference between the convex and concave sides are neglected). Accordingly, the replotted S/T profiles might be expected to coincide. However, as shown in Fig. 4(c), they have different profiles even when their diameters are the same. Thus Reuleaux and Kubota trigons do not have the same energy difference ΔE^{ST} even when they have the same confinement area $\mathcal{A}$ [see Fig. 4(b)] or the same diameter

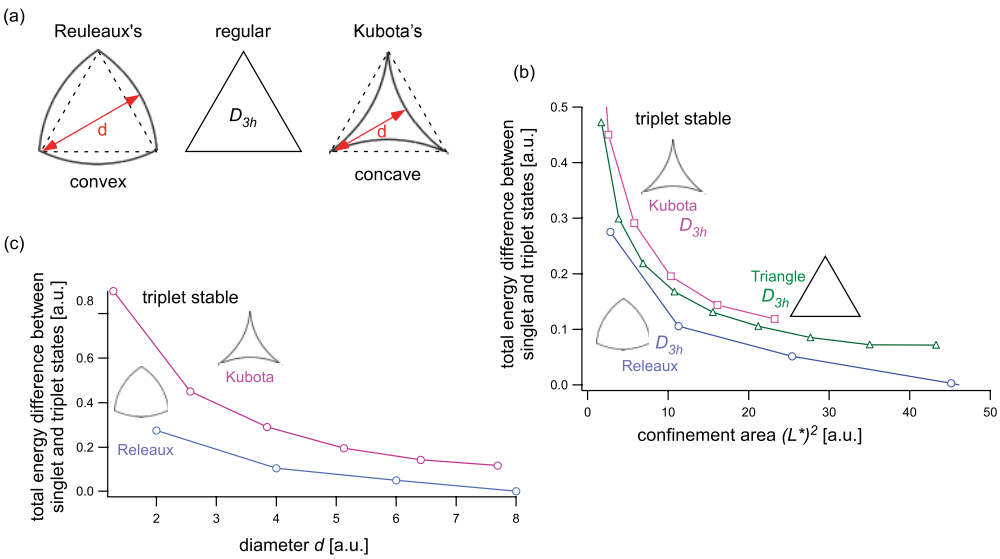

FIG. 4. (Color online) (a) Comparison of regular, Reuleaux, and Kubota trigons. Modified trigons proposed by Reuleaux and Kubota are formed by a trace of constant width distance d, but they have the same point group symmetry (D_{3h}) as a regular trigon. Kubota and Reuleaux trigons have the following relations between the confinement area $\mathcal{A}$ and width distance d: $\mathcal{A} = \frac{\pi}{8}d^2$ (Kubota) and $\mathcal{A} = \frac{1}{2}(\pi - \sqrt{3})d^2$ (Reuleaux). Accordingly, when these modified trigons have the same base length of, for example, $L = 6$, they will have different confinement areas and effective confinement lengths L^* of 5.037 (Reuleaux), 3.948 (regular), and 2.400 (Kubota). The UHF S/T profiles of these three modified trigons are shown as functions of (b) confinement area and (c) diameter d.

d [see Fig. 4(c)]. This feature indicates that the apex shape (i.e., the apex angle) is crucial for energetic stabilization because the quantum eigenstates are determined by the coherency of the wave functions confined inside.

VI. DISCUSSION

The result shown in Fig. 5 suggests an even-odd (parity) effect in the edge number. The total energy difference $\Delta E^{\mathrm{ST}} = E^{\mathrm{S}} - E^{\mathrm{T}}$ between the lowest singlet state and the lowest triplet state changes its value and sign depending on the polygon shape. Figure 5 further demonstrates that the sign is determined by the parity of the apex number: the odd polygonal QDs have stable triplet ground states so that $\Delta E^{\mathrm{ST}} > 0$, whereas ΔE^{ST} for the even polygonal QDs becomes negative, showing the anti-Hund rule. To understand the meaning of this interesting result, we need to consider necessary conditions required for this clear even-odd effect. At first, the value of $L^* = 4.968$ has to be chosen. This value is the critical confinement length L^{ST}, at which $\Delta E^{\mathrm{ST}} = 0$ is found for the circular QD of the limiting polygon. Another important point is that the result is obtained by the UHF calculation. To derive complete interpretation, we need to study L^* dependence of the ground-state multiplicity within and beyond UHF.

With an increase in L^*, the QD system changes from a weak-coupling regime to a strong-coupling regime. QDs having a large L^* approach to the classical limit, where the Coulomb energy is dominant. Let us review Fig. 3. Along the horizontal axis, the regime changes from the weak-coupling limit to the strong-coupling one. The UHF solutions shown in this figure indicate us general tendency on the singlet-triplet instability, but the detailed understanding would request much accurate description of the electronic state like the res-UHF CI method. In this discussion, instead, we give a qualitative argument. For this purpose, the strong-coupling regime, which starts from the classical limit, is convenient. The steps of our argument are composed of (1) energetics in the classical limit, (2) evaluation of the magnetic instability at this limit, (3) consideration of the quantum fluctuation effects in the strong-coupling regime, and (4) interpretation of the results in the intermediate-coupling regime.

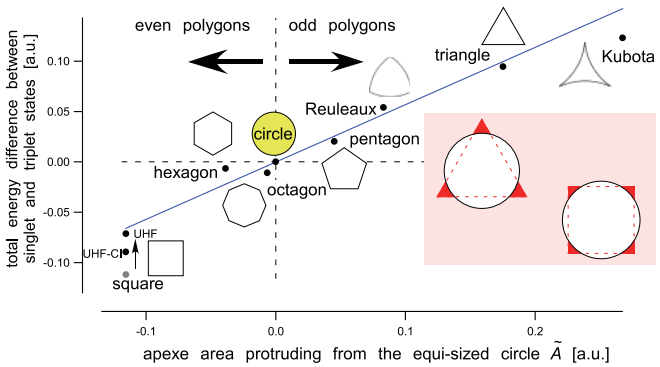

FIG. 5. (Color online) Relationship between the energy difference $\Delta E^{\mathrm{ST}} = E^{\mathrm{S}} - E^{\mathrm{T}}$ and the protruding area of the apexes $\tilde{\mathcal{A}}$ for trigons (regular, Kubota, Reuleaux), tetragon, pentagon, hexagon, octagon, and circle. The area of the apex protrusion $\tilde{\mathcal{A}}$ is defined as the area of a polygon protruding from the equisized circle (see inset). ΔE^{ST} at $L^* = 4.968$ is used to clarify the influence of the number of apexes and the parity on the total energy difference (signs of $\tilde{\mathcal{A}}$ and ΔE^{ST} are positive for odd polygons and negative for even polygons). The value $L^* = 4.968$ is the critical confinement length L^{ST} of the 2D circle [ΔE^{ST}(circle) = 0] in Fig. 3.

A. Classical limit

In the classical limit of $L^* \to \infty$, electrons behave as classical particles. Accordingly, the energy is determined only by configuration of electrons, i.e., positions of electrons in the polygonal QD. Here, we consider the hexagon as the representative example and derive qualitative discussion. The detailed discussion is given in Appendix C. Let us consider large, yet finite, L^*. In this limit, classical configuration of four electrons is determined so that they keep apart from each other in the dot as far as possible. Symmetry consideration allows us to reduce the number of possible configurations in D_{2h}, $D_{2h'}$, or D_{3h} representations of the point group D_{6h}. The highly symmetric configuration can appear as a special case of these configurations, as D_{4h} that is a special case of D_{2h} as shown in Fig. 6. We summarize the Coulomb energy of four typical symmetric configurations. The lowest one is given by $D_{2h'}$, in which two electrons locate at two opposite apices and the other two are at the centers of two edges. This configuration has the largest surrounding area among the other symmetric configurations. In contrast, we should note that the triangular configuration with the central point with the D_{3h} symmetry is energetically unstable in the hexagon.

Let us discuss the results on the Coulomb energy for allowable configurations in the other polygons. In Table I, the Coulomb energy and the area size are given for trigon, tetragon, pentagon, and hexagon. We see that trigon is the exceptional case, where the triangular configuration has lower Coulomb energy than the square configuration. The area size is also larger for the triangle than the square. In the other polygons tested, we always have the lowest Coulomb energy for the square configuration. Thus the trigon is the exceptional and we cannot find an even-odd effect in this limit.

B. Interelectron interaction and magnetic interaction

In the classical limit, the degrees of freedom in the charge distribution only determine the energetics. The magnetic multiplets should degenerate with each other as long as the charge distribution is the same. The lowest-order perturbation should appear as the magnetic interaction between localized electrons. A perturbative argument allows us to determine the lowest spin state as follows. We have typically two configurations for four-electron states. One is the square and the other is the triangle. When the square configuration is selected, the rectangle configuration allows antiferromagnetic spin alignment. Neighboring two spins align to cause an antiparallel spin configuration with two up spins and two down spins totally. Thus we can have the stable singlet configuration. When the triangle configuration causes, three electrons are located at the apices and the last electron should be at the center of the triangle arrangement. In this configuration, antiferromagnetic spin alignment for each pair of neighboring spins is allowed to have the triplet spin state. This is because

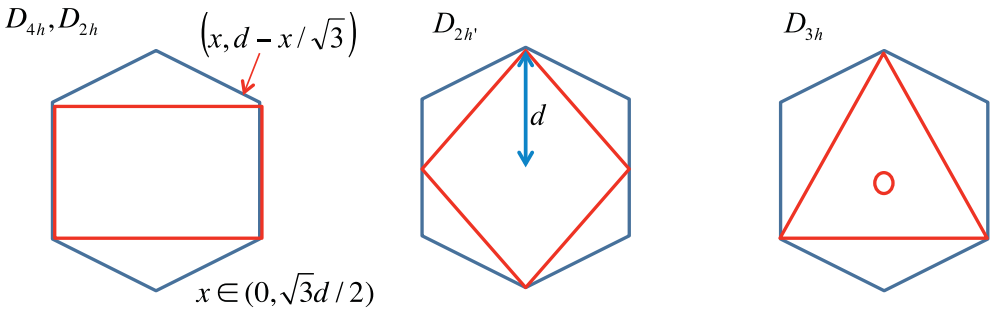

FIG. 6. (Color online) Classically possible configurations for four electrons in hexagon. Symbol d is the distance from the center to the edge.

only the center electron has a down spin opposite to the other up spins, so that residual $S_z = 3/2 - 1/2 = 1$ remains. When the electron system possesses the SU(2) rotational symmetry, the $S_z = 1$ state should appear as a highest weight state of a triplet. Thus we can say that the triplet state appears as the lowest state. Following this naive but natural argument, we conclude that the ground-state triplet appears only for the trigon, and the other polygons should show the stable singlet ground state.

Now we compare this conclusion with results in Figs. 5 and 7 to find consistency. In Fig. 3, all polygons and the circle except for the trigon go into the singlet stable phase, when L^* becomes large enough. The UHF calculation counts the Hartree energy accurately. Therefore, if we can find the square electron configuration in the singlet solution as the stable state in the large L^* limit, we can say that the picture in the classical limit holds as well. For the singlet solutions in Fig. 7(c), we indeed see the square charge distribution as the four peaks in the spin density profile of the singlet state. Furthermore, the $D_{2h'}$ configuration is found in the singlet state of the hexagon. When L^* becomes enough large, we can find the stable singlet state as the lowest scf solution of the UHF calculation.

C. Kinetic and Coulomb energies

When L^* becomes marginal, the quantum fluctuation determines the stable state to gain the kinetic energy, too. The total balance between the Coulomb interaction and the kinetic energies is maintained by creating a correlated wave function extending over the quantum dot. Let us see the spin density of the triplet states in Fig. 7(c). In the hexagon, the distribution of up electrons becomes broadened like a ring around the down electron at the center. The delocalized nature makes the kinetic energy of the triplet rather low compared to the singlet [see Fig. 7(b)].

For the evaluation of energy reduction driven by the kinetic energy, the self-consistent determination of the wave function is demanded. In this sense, the primary important step is determination of UHF solutions providing good representations of the point group symmetry. To determine energy balance between the multiplets further requires us to utilize a beyond-UHF calculation. In this sense, finding of various representations in the triplet and the singlet states shown in Fig. 7 poses a question whether the energy difference between singlet and triplet states is monotonic in L^* or not. This is exemplified by finding of the spin density of triplets in pentagon and hexagon. We have a center peak of the down spin in these polygons. The resulting charge density is not the square charge distribution, which should be energetically lower than the other configurations in the classical limit.

D. Weak coupling regime

When the kinetic energy becomes dominant in a dot with a small confinement length L^*, and if we are allowed to utilize the perturbation argument for the Hund rule, the triplet-stable phase appears in each quantum dot with four electrons. Experimentally, the triplet ground state has been often concluded for the circular quantum dot with four confined electrons.[33] Thus we can conclude existence of the

TABLE I. Singlet-triplet energetics based on the classically limited electron configuration. We evaluate the energetical stabilization of the kinetic term by the comparison of the size in square (singlet) and triangle (triplet) inscribed maximally in polygons [see Fig. 7(a)]. We also estimate the energetic stabilization due to the interelectron term by the sum of the inverse of the interelectron distance. We give those sizes and sums of the inverse of the interelectron distance for the inscribed tetragons and trigons. All the values are given by the distance from the center to the edge corners of the polygon ζ.

	Trigon		Tetragon		Pentagon		Hexagon	
	Square	Triangle	Square	Triangle	Square	Triangle	Square	Triangle
Area size/kinetic	$0.65\zeta^2$	$1.30\zeta^2$	$2.00\zeta^2$	$0.93\zeta^2$	$1.56\zeta^2$	$0.94\zeta^2$	$1.61\zeta^2(D_{4h})$ $1.73\zeta^2(D_{2h})$	$1.30\zeta^2$
$\sum_i$/Coulomb	$\frac{6.01}{\zeta}$	$\frac{4.73}{\zeta}$	$\frac{3.41}{\zeta}$	$\frac{5.60}{\zeta}$	$\frac{3.87}{\zeta}$	$\frac{5.57}{\zeta}$	$\frac{3.81}{\zeta}(D_{4h})$ $\frac{2.15}{\zeta}(D_{2h})$	$\frac{4.73}{\zeta}$

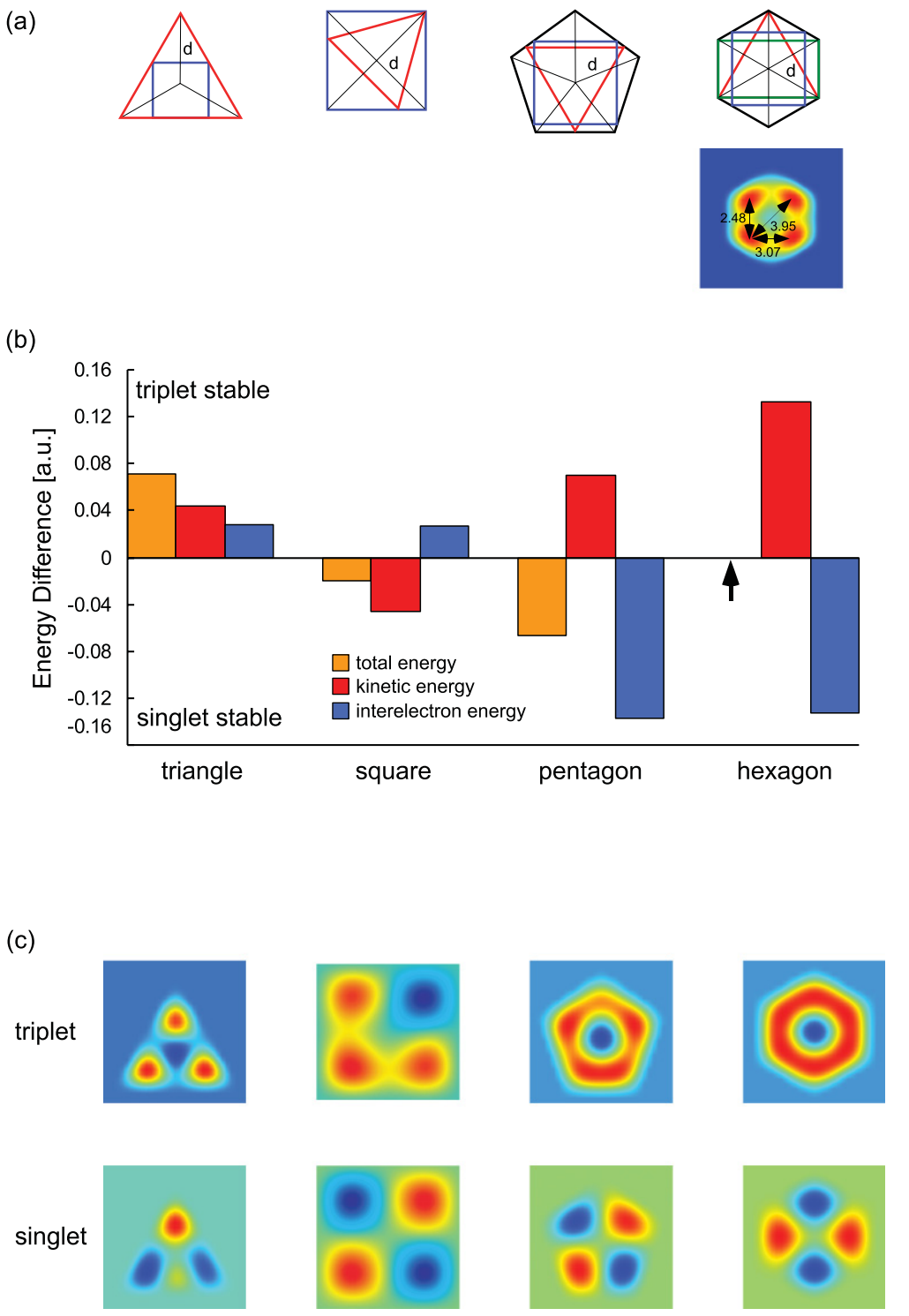

FIG. 7. (Color online) Illustration of the triangles and squares inscribed maximally in polygons of trigon, tetragon, pentagon, and hexagon (a). One should note that hexagon inscribes two types of rectangles inside; a regular square (D_{4h}) and a rectangular one (D_{2h}). We also show the energy decomposition of their total energies into the kinetic and interelectron terms (b). Those differences are calculated for those polygons having the the critical distance L^{ST} where the circle cause the S/T instability as shown in Fig. 3. Consequently, the distance from the center of the gravity to the edge corners ζ is 4.3869 for the trigon, 3.5355 for the tetragon, 3.2426 for the pentagon, and 3.1020 for the hexagon, respectively. We further show the calculated spin density of the spin singlet and triplet states for these polygons in (c). One should note that four electrons of hexagon distribute not squarely but rectangularly in the spin-singlet state, as predicted in Table I.

weak coupling regime. When we could realize larger L^* in experiment, the singlet stable phase should appear in a 2D circular dot, as the above argument suggested. The energy diagram should be much rich in the low energy owing to

near degeneracy between possible configurations. We need, however, to create a perfect 2D circular dot to realize the same physics as the simulation.

In Fig. 3, we actually see the triplet stable phase for all polygons as well as circle, when L^* is small enough. This is realization of the weak coupling regime. The stabilization energy counted in the UHF calculation is shown in this figure. However, the list of polygons in an order by the stabilization energy of the triplet ground state relative to the lowest singlet solution is trigon, octagon, pentagon, hexagon, and tetragon. This sequence is different from the order in Fig. 5 found as the even-odd effect. Thus the explanation of the even-odd effect is not easy starting from the weak-coupling regime given by UHF.

E. Intermediate regime

In the intermediate regime, we have another change in the sequence of polygons in Fig. 3. When $L^* \simeq 8$ a.u., we have trigon as the exception. Tetragon and pentagon has almost the same value of energy difference. Then, below circle, hexagon and octagon appears in Fig. 3. In addition, we have a chance to obtain several scf solutions. In the tetragon, there appear two different scf solutions for singlet states, when L^* becomes greater than 4 a.u. Appearance of multiple scf solutions suggests that it is not trivial to have a special rule for the stability of the ground state even within the UHF scheme. Therefore a clear even-odd effect found in Fig. 5 is prominent. Confirmation of the rule should be taken by experiments and simulations. If we can create a real 2D circular QD with degenerate singlet and triplet ground states, we would be allowed to confirm the rule in real experiments. Another good trial is to find res-UHF CI solutions for all the polygons. For this simulation, the solutions found in this paper would provide an informative starting point.[34]

VII. CONCLUSION

We have qualitatively (but systematically) studied the relationship between the spin multiplicity of the ground state and the morphology of 2D polygonal QDs with number of apexes M of 3 (trigon), 4 (tetragon), 5 (pentagon), 6 (hexagon), 8 (octagon), and also a circle, in terms of the MFT approaches. Odd polygons (trigon, pentagon) prefer to generate the ground-state triplet as predicted by Hund's rule, whereas even polygons (tetragon, hexagon, octagon) cause ground-state instability in the spin multiplicity and tend to produce the anti-Hund state of the ground-state singlet with strengthening of the interelectron interaction. The circle, which has an infinite number of apexes ($M = \infty$) is intermediate between these two cases. The present study provides much needed information to improve electronic structure calculation methods. If one can perform observation of polygonal QDs in an experiment, and if the ground-state multiplicity is investigated by varying L^*, determination of ΔE^{ST} would be possible. Then, the order found in Fig. 5 may be tested. If the order following the even-odd rule explained above appeared, it would suggest feasibility and relevance of UHF in the medium correlation regime.

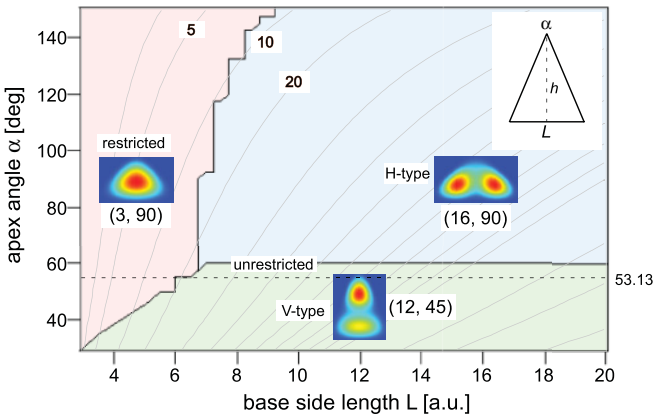

FIG. 8. (Color online) Distribution of electron density for two electrons confined in a trigon with the spin singlet. Equiarea lines of the trigon $A = \frac{L^2}{4\tan(\alpha/2)}$ and density profiles of restricted solutions and unrestricted H- and V-type solutions are also shown. The left and right numbers in the parentheses are the base line length L and the apex angle α, respectively.

ACKNOWLEDGMENTS

One of the authors (KT) would like to express his thanks to Satoshi Sasaki of NTT Basic Research Laboratory, Norikazu Tomita of Yamagata University, Richard Clark of Wasaeda University for their fruitful and constructive comments. He also would like to express his great thanks to Esa Räsänen of University of Jyväskylä for his open communication. This work was partly supported by the "High-Tech Research Center" Project for Private Universities and a matching fund subsidy from the Ministry of Education, Culture, Sports, Science and Technology (MEXT), Japan, 2008.

APPENDIX A: TWO-ELECTRON SPIN SINGLET STATE IN TRIGON

Here, we briefly discuss the electronic state of two electrons confined in a 2D trigon with the spin singlet configuration (completely unpolarized; $N^\alpha = N^\beta$). Figure 8 illustrates the electron density distributions for the UHF singlet solution as functions of the base line L and the apex angle α. Two types of SCF solutions are found: a restricted SCF solution with a nodeless density distribution and an unrestricted SCF solution with two peaks in ρ. The unrestricted solutions can be further classified into H (horizontal) and V (vertical) types. In H-type solutions, the two peaks in the electron density are located near the base line, whereas the two peak positions are aligned perpendicular to the base line in the V-type solution. These three characteristic density distributions depend on the deformation of the trigon by L and α. Therefore we qualitatively investigated these characteristic electron separation based on the relation between the interelectron term and the geometrical features of the deformed trigons.

The strong confinement causes the one-electron energy term to be greater than the interelectron one, and the individual UHF orbitals coincide irrespective of the spin polarization α and β. Thus, RHF-like solutions are obtained even in UHF calculations. The present deformation of the trigon by varying α and L maintains the point group symmetry of C_{2v} and

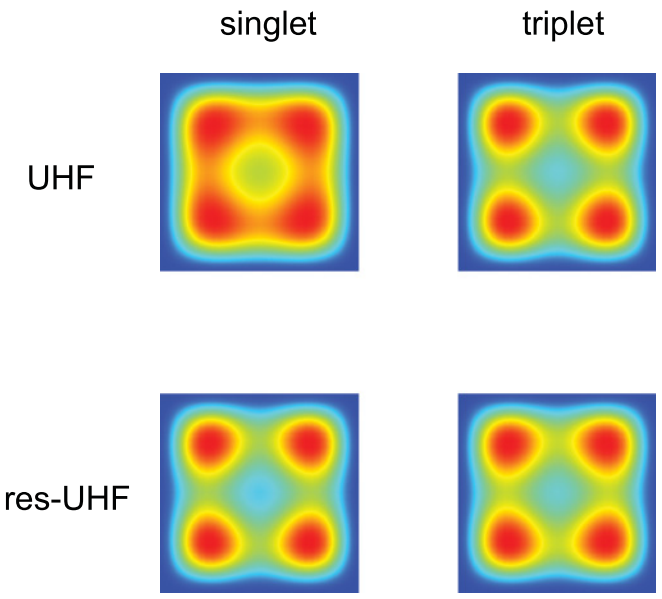

FIG. 9. (Color online) Density profiles of four electrons confined in tetragon having $L = 6$. We can compare those calculated by UHF approach with those by res-UHF treatment, in accordance with spin-singlet and spin-triplet states.

produces a confinement area of

$$\mathcal{A} = \frac{L^2}{4\tan(\alpha/2)}.$$

We show the resulting equiarea lines in Fig. 8, indicating that the equiarea line of $\mathcal{A} = 10 \sim 20$ represents the boundary between the restricted and unrestricted solutions. The boundary tail of the acute trigon is well described by this equiarea line.

Both H- and V-type solutions are unrestricted solutions are obtained from deformed trigons with large L and/or α in which the weak confinement strengthens the interelectron Coulomb term. The present system is assumed to be in the spin-singlet state and only the direct Coulomb term is considered. Consequently, the boundary between the H- and V-type UHF solutions can be explained in terms of the maximum distance in the trigon. Thus, we should compare the base line L with the height $h = \frac{L/2}{\tan(\alpha/2)}$. When the trigon is deformed by $\alpha = 2\arctan(1/2) \sim 53.13^\circ$, the resulting trigon has $h = L$ and the two electrons have equal separation in the longitudinal and transverse directions. Thus the point charge approximation predicts that the boundary between H- and V-type UHF solutions is determined by the line $\alpha = 53.13^\circ$. However, including the actual electron delocalization shifts this boundary to the line $\alpha = 60$ in the present UHF calculations, as shown in Fig. 8.

APPENDIX B: TOTAL CHARGE DISTRIBUTION

The lowest UHF scf-solution produces the quasicrystalline structure in the charge density (CD) when four electrons are confined in the tetragon having $L = 6$ (see Fig. 9). The resulting CD structure shows the fourfold rotational symmetry (C_4), whereas the corresponding UHF spin density (SD) shows the twofold symmetry. Consequently, the symmetry nature of the D_{4h} Hamiltonian is violated, as indicated in Fig. 1(b). One should note that the UHF calculation produces the other scf-solutions, being in the rotational relation by $\pi/2$ mutually. Accordingly, the res-UHF approach including these UHF solutions naturally reverts the D_{4h} symmetry even in the SD structure [see Fig. 1(c)]. This result agrees with the EDM result by Creffield *et al.*[14] who have found the similar quasicrystalline CD structure in the sufficiently larger QD. Thus the MFT approach of UHF (DFT) can give a qualitatively correct estimation in the CD distribution.

APPENDIX C: CLASSICAL LIMIT OF FOUR-ELECTRON CONFIGURATION

Neglecting the extension of the wave functions of the individual electrons [point electron approximation (PEA)], the four electrons in the spin-singlet state are classically thought to localize at the four corners, forming a regular square (D_{4h}) electron configuration with alternating spin polarization. In contrast, the four electrons in the spin-triplet state are thought to form a starlike triangle (D_{3h}) conformation; the three electrons are localized at the three corners having same spin and the remaining electron having an opposite spin at the center. That is, in the classical PEA, four electrons having a spin-singlet multiplicity prefers to distribute into a square, whereas those having a spin-triplet multiplicity tend to distribute into a triangle. Furthermore, one should remember the following two tendencies; electrons delocalized strongly reduce the energy through the kinetic term and larger separation distances reduce the Coulomb repulsion energy. Consequently, we can qualitatively discuss the singlet-triplet energetics by finding which has a larger size between the triangle and square inscribed in the polygon, because four-electron classically form a triangle or square configuration in accordance with the spin multiplicity of the triplet or singlet. In the following, we first find which has a larger size between the triangle and square inscribed in the polygon. We then predict the S/T instability classically. Finally, we decompose the UHF total energy into the kinetic and Coulomb terms and discuss the validity of the classically limited electron configuration model.

Table I compares the size of the largest triangles and squares inscribed within the polygons $M = 3$ (trigon), 4 (tetragon), 5 (pentagon), and 6 (hexagon). It is crucial to find the larger shape between the inscribed triangle and square for the individual polygons, because the larger shape causes the larger energetical stabilization through both the kinetic and Coulomb terms. When the inscribed triangle is larger than the inscribed square, the kinetic term in the spin triplet state is expected to be energetically more stable than in the spin-singlet one. Similarly, the interelectron term in the spin-triplet state is energetically more stable than in the spin-singlet one. Consequently, both the kinetic and interelectron terms preferentially cause the ground-state triplet in this case. A has an area of the inscribed triangle ($1.30\zeta^2$), being larger than that of the inscribed square ($0.65\zeta^2$). Here, ζ is the distance from the center to the edge corners of the polygon. This inscribed triangle also gives a smaller value for the sum of the inverse of the interelectron distance $4.73/\zeta$, compared with the inscribed square ($6.01/\zeta$). Consequently, the classically limited electron configurations suggest that four electrons confined in a trigon

cause a spin triplet in the ground state. Analogously, Table I indicates that four electrons confined in a tetragon or pentagon prefer a spin singlet in the ground state, because the inscribed square has a larger area than the inscribed triangle. One should further note that a hexagon can inscribe two types of squares inside: one is a square (D_{4h}) and the other is a rectangle (D_{2h}) as shown in Fig. 7(a). Table I indicates that the rectangle (D_{2h}) gives the largest area of $1.73\zeta^2$ and the smallest value of $2.15/\zeta$. Accordingly, a hexagon also is expected to cause a spin singlet in the ground state where the four electrons would distribute in a rectangle rather than square.

We now compare these simple predictions with the UHF results in Fig. 7(b). We can easily decompose the total energy of the four electrons into the kinetic and interelectron interaction terms because we employed the hard-wall potential to define the boundaries of the individual polygons. The resulting energy decomposition demonstrates that both the kinetic and interelectron terms work to cause the spin triplet state in a trigon, as predicted classically. Except for the trigon, the square is larger when inscribed in the polygons (tetragon, pentagon, and hexagon), and the ground state singlet is expected classically. Based on the numerical values of the calculated UHF total energy alone, this classical prediction might be consistent. However, the decomposed energy terms are not necessarily consistent with the classical prediction: the Coulomb term in the tetragon works to cause the spin-triplet state. In contrast, the pentagon and hexagon prefer the spin-triplet configuration because of the kinetic term. These disagreements are caused by the conflicting electron/spin distribution found in the calculated UHF solutions [see Fig. 7(c)] where a starlike triangle distribution of the spin triplet is only found in the trigon but the square and/or squarelike distribution is found in the tetragon, pentagon, and hexagon.

Comparison of results for QDs with the known results from the Hubbard model and related studies is interesting as well. The starlike triangle configuration for the triplet ground state in a trigon reminds us of the electronic state of trimethylenemethane (TMM).[32] We find that the starlike triangle configuration prefers the triplet state both in the electron gas and in the tight-binding regimes. There have been several theoretical studies using the extended Hückel approach or the Hubbard model. The half-filled four-site Hubbard model on a starlike graph shows the triplet ground state with local antiferromagnetic correlation. This ferromagnetic ground state is understood by a ferromagnetic spin configuration appearing in the Heisenberg antiferromagnetic spin model on the same graph. Thus the strong-correlation regime of the trigonal QD is comparable, or essentially identical to the corresponding Hubbard model. In this respect, advantage of the QDs is found. Now, we consider a final message on this advantage in the controllability as follows. The semiconductor quantum dot is known to be controlled by applied bias voltage. There are several techniques to fabricate control gates on the substrate supporting the dot. If we have a QD in a Reuleaux triangle, the creation of three surrounding gates and the application of a bias may shift the electronic character in a Kubota triangle. Accordingly, the stability of the triplet ground state is expected to be enhanced by this bias voltage. Therefore by utilizing the results found in this paper, we can hope to design controllable QDs.

*takeda@waseda.jp

[1] M. A. Kastner, Phys. Today **46**, 24 (1993).

[2] S. Tarucha, D. G. Austing, T. Honda, R. J. van der Hage, and L. P. Kouwenhoven, Phys. Rev. Lett. **77**, 3613 (1996).

[3] For a review, e.g., *Quantum Dots*, edited by L. Jacak and A. Wójs (Springer, Berlin, 1998).

[4] For a review, e.g., *Quantum Dot Heterostructures*, edited by D. Bimberg, M. Grundmann, and N. N. Ledentsov (Wiley, Chichester, 1999).

[5] A. Harju, E. Räsänen, H. Saarikoski, M. J. Puska, R. M. Nieminen, and K. Niemela, Phys. Rev. B **69**, 153101 (2004).

[6] E. Räsänen, H. Saarikoski, M. J. Puska, and R. M. Nieminen, Phys. Rev. B **67**, 035326 (2003).

[7] G. W. Bryant, Phys. Rev. Lett. **59**, 1140 (1987).

[8] For a review, e.g., S. M. Reimann and M. Manninen, Rev. Mod. Phys. **74**, 1283 (2002).

[9] M. Koskinen, M. Manninen, and S. M. Reimann, Phys. Rev. Lett. **79**, 1389 (1997).

[10] A. W. Overhauser, Phys. Rev. Lett. **4**, 462 (1960); Phys. Rev. **128**, 1437 (1962); **167**, 691 (1968).

[11] C. Yannouleas and U. Landman, Phys. Rev. Lett. **82**, 5325 (1999).

[12] K. Hirose and N. S. Wingreen, Phys. Rev. **59**, 4604 (1999).

[13] D. G. Austing, S. Sasaki, S. Tarucha, S. M. Reimann, M. Koskinen, and M. Manninen, Phys. Rev. B **60**, 11514 (1999).

[14] C. E. Creffield, W. Häusler, J. H. Jefferson, and S. Sarkar, Phys. Rev. B **59**, 10719 (1999).

[15] C. E. Creffield, J. H. Jefferson, S. Sarkar, and D. L. J. Tipton, Phys. Rev. B **62**, 7249 (2000).

[16] E. Räsänen, H. Saarikoski, V. N. Stavrou, A. Harju, M. J. Puska, and R. M. Nieminen, Phys. Rev. B **67**, 235307 (2003).

[17] E. Räsänen, A. Harju, M. J. Puska, and R. M. Nieminen, Phys. Rev. B **69**, 165309 (2004).

[18] E. Räsänen, PhD thesis, Helsinki University of Technology, Finland, 2004.

[19] For the spin-singlet state for those 2D polygons (3, 4, 5, and 6), Räsänen *et al.*[17] have carefully studied the electronic structures. They assumed "spin singlet" and calculated the symmetry-preseved DFT ($n_\alpha = n_\beta$) and symmetry-broken SDFT ($S_z = 0$) ground states in order to reveal the Wigner molecule formation.

[20] 2D polygonal and circular QDs generate characteristic single-electron states that can be classified by two quantum numbers. For example, the single-electron states generated by circular QDs can be classified by the radial (n) and angular (l) quantum numbers. Each single-electron state with quantum number n is doubly degenerate due to the two values of $\pm l$ resulting from clockwise and anticlockwise rotations about the C_∞ axis.

[21] P. Hohenberg and W. Kohn, Phys. Rev. **136**, B864 (1964).

[22] W. Kohn and L. J. Sham, Phys. Rev. **140**, A1133 (1965).

[23]T. Okunishi, Y. Negishi, M. Muraguchi, and K. Takeda, Jpn. J. Appl. Phys. **48**, 125002 (2009).

[24]Y. Negishi, T. Okunishi, M. Ishizuki, and K. Takeda, Jpn. J. Appl. Phys. **50**, 085001 (2011).

[25]As for the density functional theory, adopting the spin-dependent mean-field approach, i.e., the local spin density approximation (LSDA), allows us to have the spin-density as a self-consistently determined order parameter. Each polygonal QD, however, is a finite system. Therefore the description of LSDA is not expected to be suitable for the finite quantum system, since the total energy of the electron system is given as a functional of the spin density. We know that the spin density should be always zero for the totally singlet state. However, LSDA solutions for a finite system in a correlated regime can show an Ising-like density profile. This behavior is similar to the UHF approach. To represent magnetism in a finite quantum system, we are requested to implement a multireference density functional theory. For this purpose, characteristic behavior of LSDA solutions should be analyzed, since the results are to be utilized to expand the basis of many-body states in a CI representation. The location of the critical point on the L axis in Fig. 1 is important for this analysis of DFT.

[26]S. Akbar and In-Ho Lee, Phys. Rev. B **63**, 165301 (2001).

[27]H. Fukutome, Prog. Theor. Phys. **80**, 417 (1988).

[28]N. Tomita, A. Ikawa, and H. Fukutome, J. Phys. Soc. Jpn. **62**, 4338 (1993).

[29]N. Tomita, A. Ikawa, and H. Fukutome, J. Phys. Soc. Jpn. **63**, 191 (1994).

[30]The Ising Hamiltonian ($\mathcal{E}_{\text{Ising}}$) is defined as

$$\mathcal{E}_{\text{Ising}} = \sum_{i<j}\sum(-K_{ij})S_i^z \cdot S_j^z = (-K_0)\sum_{i<j}\sum\frac{1}{R_{ij}}S_i^z \cdot S_j^z.$$

In the calculation of the value $\mathcal{E}_{\text{Ising}}$, we employ the peak-hight approach and the effective exchange term K_{ij} is approximated by the inverse of the interpeak distance R_{ij}. The calculated energy is $1.04K_0$ for the spin singlet and $0.53K_0$ for the spin triplet, and is naturally consistent with the Hund prediction because of the positive value of K_0.

[31]T. Ezaki, N. Mori, and C. Hamaguchi, Phys. Rev. B **56**, 6428 (1997).

[32]W. T. Borden, H. Iwamura, and J. A. Berson, Acc. Chem. Rev. **27**, 109 (1994).

[33]R. Hanson, L. P. Kowenhoven, J. R. Petta, S. Tarucha, and L. M. K. Vandersypen, Rev. Mod. Phys. **79**, 1217 (2007).

[34]When we can find charge distribution with four peaks in a QD, we can safely say that the system is in a strong-coupling regime. The Wigner crystallization has been often reported in dilute systems. If the system is in the crystalized state, we would be able to see the singlet for the circular QD. Once we can realize the singlet phase in the circular dot, we immediately are able to design a controllable quantum dot. Let us suppose that three dos are created around a circular QD. By applying bias voltages to the surrounding dots, we can introduce additional confinement potential to realize a modified QD. The center dot may be close to a Kubota dot pictured in Figs. 4 and 5. Using this QD systems, we can realize a transition from the singlet-stable to the triplet-stable phase in the center dot.